

Fast Determination of Phosphorus Concentration in Phosphogypsum Waste Using Calibration-Free LIBS in Air and Helium

Khaled Elsayed

Imam Abdulrahman Bin Faisal University College of Engineering

Walid Tawfik (✉ walid_tawfik@niles.edu.eg)

Cairo University National Institute of Laser Enhanced Sciences <https://orcid.org/0000-0002-1675-4187>

Ashraf E M Khater

Egyptian Atomic Energy Authority

Tarek S Kayed

Imam Abdulrahman Bin Faisal University College of Engineering

Mohamed Fikry

Cairo University Faculty of Science

Research Article

Keywords: Phosphorus, Phosphogypsum, Laser-induced breakdown spectroscopy, Helium, Calibration-free, Electron Temperature, Electron Density

Posted Date: April 16th, 2021

DOI: <https://doi.org/10.21203/rs.3.rs-314020/v1>

License:  This work is licensed under a Creative Commons Attribution 4.0 International License.

[Read Full License](#)

Version of Record: A version of this preprint was published at Optical and Quantum Electronics on January 4th, 2022. See the published version at <https://doi.org/10.1007/s11082-021-03474-x>.

Abstract

This work represents a novel method to determine phosphorus (P) concentration in phosphogypsum (PG) waste samples using calibration-free laser-induced breakdown spectroscopy (LIBS). A 50 mJ Q-switched Nd: YAG laser has generated the PG LIBS spectrum. Spectroscopic analysis of plasma evolution has been characterized by electron density N_e and electron temperature T_e using the emission intensity and Stark broadening for P I characteristic lines 213.61, 214.91, and 215.40 nm under non-purged (air) and purged (helium) conditions. It was found that both T_e and N_e have significant changes linearly with P concentrations 4195, 5288, 6293, and 6905 ppm. The values of plasma T_e and N_e increased from about 6900 to 10000 K and 1.1×10^{17} to $3.4 \times 10^{17} \text{ cm}^{-3}$, respectively, for the non-purged PG. On the other hand, T_e and N_e ranged from 8200 to 11000 K and 1.4×10^{17} to $3.5 \times 10^{17} \text{ cm}^{-3}$, respectively, for the PG purged with helium. It is concluded that T_e and N_e values represent a fingerprint plasma characterization for a given P concentration in PG samples, which can be used to identify P concentration without a PG's complete analysis. These results demonstrate a new achievement in the field of spectrochemical analysis of environmental applications.

1. Introduction

One of the significant nutrients is phosphorus (P), as well as nitrogen (N) and potassium (K), which are essential for plant growth and crop production. Phosphorus deficiency in agricultural soil can be overcome using phosphate bearing fertilizers (Kaski et al. 2003). Phosphate ore is a crucial source for phosphate fertilizers and phosphorus for agricultural applications. Phosphate fertilizers' life cycle starts with phosphate ore (mainly of sedimentary or ingenious origin) that is chemically treated with sulphuric acid to produce phosphoric acid and phosphogypsum (PG) (CaSO_4) as a by-product waste. PG waste has considerable concentrations of radioactive materials (^{238}U , ^{226}Ra , ^{210}Pb , ^{232}Th , and others), phosphorus pentoxide (P_2O_5), and some trace elements such as chromium, fluoride, zinc, antimony, arsenic, lead, cadmium, and copper (Calin et al. 2015; Cuadri et al. 2014; Potiriadis et al. 2011). So, a precise determination of phosphate content in fertilizers and PG is needed for agricultural good-practice and environmental protection.

Phosphogypsum (PG) is a by-product waste of phosphoric acid (H_3PO_4)/phosphate fertilizers manufacture where phosphate ore attacked by sulfuric acid (H_2SO_4) as shown in the following reaction equation (Calin et al. 2015; Cuadri et al. 2014; Potiriadis et al. 2011);



(Fluorapatite) (PG)

Although there are various useful applications (such as agricultural and building materials), only about 15% of some billion tons of PG produced worldwide are recycled due to its impurities and contaminants (Nizevičienė et al. 2018; Pacheco-Torgal et al. 2012).

Recently Elisha J. J. investigated the elemental composition of nine randomly selected inorganic fertilizers using X-ray fluorescence spectrometric technique (XRF) (J. J 2014). They analyzed some fertilizers purchased from Samaru Zaria for some toxic elements (Cr, Ni, Si, V, and Zn). Even though the obtained results confirm that the elemental concentrations were within the agricultural soils ranges, they failed to detect phosphate concentrations fluctuation. Raven and Loeppert evaluated trace elements and heavy metals in a wide variety of fertilizers and soil amendments by using both Atomic Absorption Spectrometry (AAS) and Inductively-Coupled Plasma Induced Emission Spectrometry (ICP-MS) (Raven and Loeppert 1997). İlknur ŞEN used near-infrared reflectance technique to analyse soil-fertilizer mixtures on-line (Şen 2003). The method was useful for use by farmers in the field without the need to collect samples and send them to the laboratory.

The use of high-power lasers as a spectroscopic analytical tool depends on vaporization, excitation, or ionized atoms/molecules from the material surface when a laser pulse is focused on it. The atomic emission spectroscopic study of emission lines from the induced plasma can give information about the investigated material's chemical composition. This technique of spectroscopic studies is known as Laser-Induced Breakdown Spectroscopy (LIBS). LIBS is typical atomic emission spectroscopy where a high power laser pulse strikes the sample surface to produce a plasma, which will then generate a unique fingerprint for the elemental content in the sample using their characteristics lines (Ahmed et al. 2020; Farooq et al. 2020; Farooq et al. 2018; Tawfik et al. 2015a).

LIBS is suitable for quick, real-time analysis (on-line), low cost, friendly, sensitive, and high spatial resolution analysis. The samples used in LIBS are free from any progressive digestion or extraction chemicals nor strong acids. The sensitivity of LIBS technique is a critical factor, representing the enhancement of the detection limit of a minimal concentration of trace elements in the samples (Fikry et al. 2020b; Fikry et al. 2020a; Rai et al. 2001; Yueh et al. 2002). Calibration free-LIBS analysis was proposed by Ciucci *et al.* (Ciucci et al. 1999), which can be applied to any element in the periodic table provided that the physics of the plasma process and local thermal equilibrium for the observed relevant spectral information under thin plasma conditions are experimentally validated (Tawfik and Mohamed 2007).

One of the most comfortable and cheapest techniques has been utilized to enhance the sensitivity of LIBS system is purging the sample with inert gases. This improves the plasma electron temperature and density which brings back the affirmation on the sensitivity and intensity of the induced breakdown spectrum (Kaski et al. 2003; Li et al. 2018).

Fertilizers from Saudi Arabia were analyzed using the LIBS technique (Farooq et al. 2012) to detect phosphorous, manganese, magnesium, molybdenum, iron, titanium, nickel, vanadium, calcium, cobalt, cadmium, tin, sulphur, aluminium, chromium, lead, and uranium. A relatively high concentration of health-hazardous elements such as Cd, Ni, and Pb were noticed. Gallou *et al.* (Gallou et al. 2009) used a portable LIBS system to detect elements such as F, Cl, P and U on-site. A quantitative method dedicated to determining phosphorus in fertilizers of different matrix compositions using the LIBS technique was

developed. Phosphorus quantification in organic and inorganic fertilizer samples in Brazil was achieved with approximately 15% precision compared to other measurement techniques such as ICP (Marangoni et al. 2016). The LIBS technique was also used to assess agricultural products and precision agriculture compared to a standardized chemical analysis method. In their experiment, soil samples classified as thermic, fine-silty, and mixed from grassland and uplands in Tennessee (USA) were collected and smashed. The samples were analyzed using LIBS in the spectral range from 200 to 600 nm using a 532 nm Nd: YAG laser, 25 mJ pulse energy, 5 ns pulse width, with 10 Hz repetition rate. They stressed the necessity to enhance LIBS's measurement and prediction accuracy by improving the pre-treatment process, standard reference soil samples, and measurement method for a reliable quantification method (Cremers et al. 2001).

In this work, the calibration-free LIBS technique has been used to directly measure phosphorus concentrations in different phosphogypsum samples. In doing so, spectroscopic analysis of plasma evolution of laser-produced plasma has been characterized by elemental content spectra, plasma electron density, and electron temperature assuming the Local Thermodynamic Equilibrium (LTE) and optically thin plasma conditions under air (non-purge) and helium gas (purge) to enhance the LIBS signal.

2. Methodology

2.1 Sample Preparation

The phosphogypsum samples were collected from the Rad Al-Khair chemical complex on the Arabian Gulf coast - Saudi Arabia. The samples were dried in an oven at 80 °C for about 48 h, then mechanically crushed in a ball mill, and sieved through a 1mm mesh sieve. The samples were then pressed to produce tight, compact pellets with a diameter of 40 mm and a thickness of 10 mm under 200 MPa pressure for 5 min by a hydraulic oil press. The samples were pressed as pellets to decrease the sample's surface roughness, which enhanced the mass ablation's uniformity (Edwards and Winefordner 2007).

2.2 Analytical Methods

Phosphogypsum samples were analyzed for various major and minor oxides' decomposition and their concentrations in the "Australian Laboratory Services' ALS Geochemistry limited company" labs. The analysis was done by using the technique of lithium metaborate fusion digestion inductively coupled plasma-atomic emission spectroscopy ICP-AES (ALS Geochemistry method ME-ICP06). In addition to that, the Thermal decomposition Furnace or TGA (OA-GRA05 or ME-GRA05) was performed.

2.3 LIBS Setup

The laser-induced plasma (LIBS) system used in this study is the LIBS lab system (LTB Laser Technik Berlin GmbH) having the technical details shown previously elsewhere (Harmon et al. 2019; Ji et al. 2017; Merk et al. 2015). Briefly, in the current system, a Q-switched Nd:YAG laser (Quantel Ultra 50) beam with a 50 mJ laser pulses with pulse duration 5 ns at its fundamental wavelength 1064 nm, and adjustable repetition rate up to 30 Hz. The laser pulse energy was adjusted by changing the Q-switch delay using

Sophi 64 bit software designed to control the spectrometer and the whole LIBS system. The light emitted by the plasma emissions at the focal volume was collected by a set of optics and focused on an optical fiber head. This fiber bundle delivered the light to an ARYELLE 200 butterfly spectrometer. ARYELLE 200 is an Echelle spectrometer with a pre-monochromator and active wavelength stabilization. The ARYELLE 200 provides a spectral resolving power 75000–150000 and spectral resolution from 13.8 to 37.5 pm over a wavelength range 192–750 nm displayable in a single spectrum in two spectral ranges (UV and Vis). The dispersed light from ARYELLE 200 was then detected by a gateable intensified charge-coupled detector ICCD (Andor I-Stare).

The emission spectra display, processing, and analysis were done using 2D and 3D Gram/32 software programs (National Instruments, USA). In addition to the atomic database used by the mentioned software's atomic database, spectral line identification was checked by the most up-to-date electronically published database (Kramida and Ralchenko 2018).

The gate width and delay time have been chosen after performing an optimization procedure for maximizing spectral line intensity. The choice of the optimum gate width and delay time values for the spectroscopic data acquisition was accomplished by a computer-controlled system. The gate and delay times were adjusted at 1.5 and 0.8 μs , respectively. To improve the LIBS precision, spectra from 50 laser shots were averaged to reduce the statistical error due to laser shot-to-shot fluctuation. Measurements at new locations on the sample surface were taken to avoid problems linked to sample heterogeneity. Fifty laser shots were fired at each location and saved in separated files, and the average was computed and saved to serve as the library for each spectrum. The plasma emission spectra were collected in both air and helium environment by purging the sample with a helium gas flow. These processes take just a few seconds to identify the whole LIBS spectrum for the studied elemental analysis.

3. Result And Discussion

3.1 LIBS Spectrum Studies

The qualitative analysis of the phosphogypsum samples was observed from the optical spectra established from the LIBS technique using 50 laser accumulated shots of NIR nanosecond Nd: YAG pulsed laser with 5 ns pulse duration and 5 mJ pulse energy, detected on 1.5 μs gate time, 0.8 μs delay. Figure 1 (a,b) represents high-resolution LIBS emission spectra of the non-purged and purged with the He gas on phosphogypsum samples with phosphorus concentrations 4195, 5288, 6293, and 6905 ppm, respectively. All the spectra were recorded under identical experimental conditions. The spectral region from 213–216 nm is selected because it gathers the highest phosphorus emission lines intensities proposed to be under optically-thin plasma in LTE as a crucial condition for the plasma calculations parameters. The three selected lines of singly ionized phosphorus (P I) are 213.61, 214.91 and 215.40 nm due to the transitions $(3s^23p^3, ^2D_{5/2} \rightarrow 3s^23p^2(^3P)4s, ^2P_{3/2})$, $(3s^23p^3, ^2D_{3/2} \rightarrow 3s^23p^2(^3P)4s, ^2P_{1/2})$, and $(3s^23p^3, ^2P_{3/2} \rightarrow 3s^23p^2(^1D)4s, ^2D_{5/2})$, respectively. These lines were selected to study the spectroscopic

breakdown parameters since they showed the highest correlation values covering the UV wavelength range 213 to 216 nm (Marangoni et al. 2016).

The transitions' parameters of the selected P emission lines have been recognized with the NIST database's help, as demonstrated in Table 1. These data were used to evaluate the breakdown spectroscopic parameters (Kramida and Ralchenko 2018).

3.2 Concentration Calibration Studies

The LIBS concentration calibration curves of the P I spectral lines 213.61, 214.91, and 215.40 nm for phosphogypsum samples in air and purged with He gas at NIR (1064 nm) laser pulse energy 50 mJ are shown in Fig. 2. The calibration curves validate the linear increase in the LIBS signal intensity of the different LIBS spectra wavelengths with the increase of the P concentration at a high correlation coefficient $\sim 0.975 \pm 0.05$. The increase in the concentration of the P in the target ablated volume leads to an increase in the ablated mass (Galbács 2017; Qi and Lai 2012; Raciukaitis et al. 2008), which produced an increase in the absorbed laser pulse energy as given by Eq. (1), which is a semi-empirical model given by G. Raciukaitis *et al.*, in addition to H. Qi and H. Lai (Qi and Lai 2012; Raciukaitis et al. 2008).

$$m = \rho V = \rho \frac{\pi w^2 d_0}{4} \left(\ln \frac{2E_p}{\pi w^2 F_{p,c}} \right)^2 \quad (1)$$

where V is the ablation volume per a single shot pulse, ρ is the solid target density, w is the beam waist of the laser beam at the target surface, d_0 is the effective absorption depth of the target, E_p is the laser pulse energy, $F_{p,c}$ is the critical threshold fluence of the laser.

It worth noting that it has been found that in LIBS experiments under LTE conditions, an increase in the target ablated mass may lead to an increase in the plasma electron temperature and density (Fikry et al. 2020b; Fikry et al. 2020a). This plasma profile will be verified for LIBS of phosphogypsum samples under the studied conditions.

The observed linear calibration relation, as shown in Fig. 2, confirms the absence of the plasma self-absorption and assures the plasma's homogeneity (Palleschi 2020; Sabsabi 2007). The purged samples with the He gas indicated the same trend with an increase of the P concentration at the same laser pulse energy with an enhancement of the signal intensity, especially at the low sample concentrations (Kaski et al. 2003). The small concentrations enhanced approximately to the dappled (Li et al. 2018).

3.3 Breakdown Spectroscopy Parameters and Calibration-free Studies

The plasma electron temperature and density are considered as the most critical parameters of the breakdown spectroscopy studies (Ahmed et al. 2020; Farooq et al. 2020; Farooq et al. 2018; Farooq et al. 2015; Tawfik et al. 2015b). The plasma temperature is measured under the local thermodynamic equilibrium and optically-thin plasma conditions depending on the previously obtained results of the concentration calibration curve. These conditions will be confirmed later. According to these conditions, the intensities of different fertilizing samples emission lines, consider emitted from electron collisions, are much larger than from the radiative processes (Gojani 2012). It is worth noting that the reabsorption effects of plasma emission are negligible (Liu et al. 1999; El Sherbini et al. 2005). Under the LTE conditions, the Boltzmann plot method is given by (Alhijry et al. 2020; Liu et al. 1999);

$$\ln \frac{I\lambda}{A_{ki}g_k} = -\frac{1}{KT_e} E_k + \frac{FC}{U(T)} \quad (2)$$

where I is the intensity of the spectral line, λ is the wavelength of a spectral line, K is the Boltzmann constant, $U(T)$ is the partition function, A_{ki} is the transition probability, g_k is the statistical weight for the upper level, E_k is the excited level energy, T_e is the temperature, F is an experimental factor and C is the species concentration.

Fig. 3 represents Boltzmann plots for non-purged and purged samples by helium gas for P I lines (213.61, 214.91, and 215.40 nm) at 1064 nm laser wavelength and pulse energy 50 mJ. The $\ln(I\lambda/A_{ki}g_k)$ is considered for each exciting level energy E_k under a gradual increase in the P concentration values from 19200 to 3800 ppm. From equation (2), the electron temperature can be determined from each line's slope in Fig. 3, with an uncertainty of about $\pm 5\%$ (Fikry et al. 2020b; Fikry et al. 2020a).

The plasma electron density is considered for the Stark-broadening profile of P I line 213.61 nm because it has the highest correlation-coefficient (~ 0.98) with the concentration. The linewidth $\Delta\lambda_{FWHM}$ is calculated by deconvolution of the phosphorus spectral line profile as a Voigt profile (Alhijry et al. 2020; Fikry et al. 2020a) using Origin software version 9.5 at fixed laser pulse energy at 50 mJ as represented in Fig. 4.

As indicated in Fig. 4, the spectral line FWHM of the P 213.61 nm ranged from 0.02209 to 0.03588 nm with an average error ± 0.00175 nm and from 0.02337 to 0.03653 with an average ± 0.00125 nm for the non-purged and purge, respectively. The spectral line FWHM of the P I 213.61 nm under purged with He gas is larger than the non-purged condition, indicating that the purge enhanced the electron density, which verifies by calculating the plasma electron density.

The electron density is measured by the Boltzmann distribution of the electron density as in following in equation (3), considering the LTE conditions as referred before (Fikry et al. 2020b; Mortazavi et al. 2014):

$$N_e \approx \left(\frac{\Delta\lambda_{FWHM}}{2 W_e} \right) \cdot 10^{16} \quad (3)$$

where N_e the electron density (in cm^{-3}), $\Delta\lambda_{FWHM}$ the fundamental line width at half maximum, and W_e the electron Stark-broadening value. The average value of W_e for P I 213.61 nm was obtained from H. R. Griem's book (1964) as 0.00295 \AA (Griem 1964). The Stark line width $\Delta\lambda_{FWHM}$ can be corrected by subtracting the instrumental $\Delta\lambda_{instrument}$ (~ 15 pm) from the observed line width $\Delta\lambda_{observed}$ as follows:

$$\Delta\lambda_{FWHM} = \Delta\lambda_{observed} - \Delta\lambda_{instrument} \quad (4)$$

The electron temperature and the electron density calibration curves are directly proportional to the P concentration for the phosphogypsum samples under non-purged and purged He conditions, as shown in Fig. 5. The electron temperatures are found to be ranged from about 6900 to 10000 K and from 8200 to 11000 K, for the non-purged, and purged samples, respectively. On the other hand, the electron density of the non-purged and purged samples are ranged from about 1.1×10^{17} to $3.4 \times 10^{17} \text{ cm}^{-3}$ and from 1.4×10^{17} to $3.5 \times 10^{17} \text{ cm}^{-3}$, respectively.

These observations indicated an increase in the plasma electron temperature and density with the phosphorus concentration in the target samples due to the ablation mass increment, which agrees with the previous foundations (Fikry et al. 2020b; Fikry et al. 2020a; Galbács 2017; Qi and Lai 2012; Raciukaitis et al. 2008), as discussed above in equation (1). The above results clarify that the ambient plasma conditions (Air or He) play an essential role in the plasma emission characteristics. The plasma expansion rate and the background absorption for the laser energy depend on the ionization energy of the plasma surrounded gas. The main air gases are oxygen and nitrogen, which have ionization energies 13.62 and 14.53 eV, respectively, which are relatively smaller comparing with 24.58 eV for He gas (Camacho et al. 2011; Eseller et al. 2012; Kim and Desclaux 2002; Unnikrishnan et al. 2010; Welander 1898; Zvilopulo et al. 2005) According to that, then in the case of non-purge (air), the background absorbed more laser energy than in the case of purge (He) (Akram et al. 2017; Effenberger and Scott 2010; Farooq et al. 2014; Rajavelu et al. 2020). These results facilitate the opportunity to directly identify the phosphorus concentration in any unknown phosphogypsum sample by determination of T_e and N_e values for that sample; then the P concentration can be observed directly from linear curves in Fig. 5 without needing to complete analysis of the sample or building its calibration curves. The latter represents a novel calibration-free LIBS method to identify the P concentration in unknown phosphogypsum waste samples.

Finally, the verify of the LTE condition, the minimum critical electron density, proposed by McWhirter equation (5), which consider the collisional processes are dominated over the radiative processes, has been considered as following (Fikry et al. 2020a; Liu et al. 1999):

$$N_e \geq 1.6 \times 10^{12} \times \Delta E^3 \times T_e^{(1/2)} \quad (5)$$

where ΔE is the highest energy difference between the upper and the lower energy level (from Table 1 $\Delta E = 3.816$ eV) and T_e is the plasma temperature (from Fig. 5 for non-purged $T_e = 10153.1$ K, purged $T_e = 10955.3$ K). The RHS of equation (5), represents the critical N_e 8.9×10^{15} cm⁻³ for non-purged and 9.3×10^{15} cm⁻³ for the purged samples. On the other hand, the P I line's observed electron density values were in the range of 10^{17} cm⁻³ as shown in Fig. 5. Thus, the McWhirter condition is valid, which indicates that the studied plasma can be considered in the LTE condition.

From the results of the linear fitting of Fig. 5, new empirical formulas can be derived with a high correlation coefficient $\sim (0.975 - 0.985) \pm 0.05$. These formulas can be used to identify the unknown P concentration by estimate the plasma parameters (T_e and N_e) using the LIBS method under the above mentioned experiment conditions (1064 nm Nd: YAG laser, 50 mJ pulse energy, 5 ns pulse width, 30 Hz repetition rate, 1.5 μ s gate time, 0.8 μ s delay time, 50 laser shots, and at the LTE condition). Equations 6 and 7 for the non-purged, 8 and 9 for the He purged which given as follows;

for the non-purged P samples

$$T_e(K) \simeq 2.22 \times 10^3 + 1.14 \times 10^3 \times C(ppm) \quad (6)$$

$$N_e(cm^{-3}) \times 10^{17} \simeq -2.65 + 0.845 \times C(ppm) \quad (7)$$

For the He purged samples

$$T_e(K) \simeq 4.56 \times 10^3 + 9.19 \times 10^2 \times C(ppm) \quad (8)$$

$$N_e(cm^{-3}) \times 10^{17} \simeq -1.92 + 0.767 \times C(ppm) \quad (9)$$

4. Conclusion

The calibration-free LIBS was used to determine P concentration in any unknown phosphogypsum waste sample directly in the air and helium environment. The plasma electron temperature and density for the known phosphorus concentrations in different phosphogypsum samples were studied. Helium gas purging of the target surface enhanced the LIBS spectrum, plasma electron temperature, and electron density due to the increased mass ablation. The increase in the phosphorus concentration in the phosphogypsum samples from 4195 to 6905 ppm change electron temperature values ranged from about 6900 to 10000 K and from 8200 to 11000 K for samples with non-purged and purged with helium conditions, respectively. While the electron density values ranged from 1.1×10^{17} to 3.4×10^{17} cm⁻³ and 1.4×10^{17} to 3.5×10^{17} cm⁻³ for samples under non-purged (air) and He purged conditions, respectively. The observed results indicate that it is possible to improve the exploitation of calibration-free LIBS in the on-line environmental monitoring by following up only plasma parameters of the phosphogypsum to identify phosphorus concentrations without needing to thoroughly analyze the phosphogypsum, which saves a lot of time and efforts.

Declarations

Acknowledgments

This work was funded by the Deanship of Scientific Research at Imam Abdulrahman Bin Faisal University, Dammam, in Saudi Arabia under project 2016-362-Eng.

References

- Ahmed, N., Liaqat, U., Rafique, M., Baig, M.A., Tawfik, W.: Detection of toxicity in some oral antidiabetic drugs using LIBS and LA-TOF-MS. *Microchem. J.* 155, 104679 (2020).
<https://doi.org/10.1016/j.microc.2020.104679>
- Akram, M., Bashir, S., Rafique, M.S., Hayat, A., Mahmood, K.: Laser Induced Surface Morphology of Molybdenum Correlated with Breakdown Spectroscopy. *Plasma Chem. Plasma Process.* 37, 287–304 (2017). <https://doi.org/10.1007/s11090-016-9752-z>
- Alhijry, I.A., EL Sherbini, A.M., EL Sherbini, T.M.: Measurement of deviations of transition probability of the neutral silver lines at 827.35 and 768.77 nm using OES-technique. *J. Quant. Spectrosc. Radiat. Transf.* 106922 (2020). <https://doi.org/10.1016/j.jqsrt.2020.106922>
- Calin, M.R., Radulescu, I., Calin, M.A.: Measurement and evaluation of natural radioactivity in phosphogypsum in industrial areas from Romania. *J. Radioanal. Nucl. Chem.* 304, 1303–1312 (2015).
<https://doi.org/10.1007/s10967-015-3970-3>
- Camacho, J., Sol, L.D., Santos, M., Juan, L.J., Poyato, J.: Optical Breakdown in Gases Induced by High-power IR CO₂ Laser Pulses. *undefined.* (2011)
- Ciucci, A., Corsi, M., Palleschi, V., Rastelli, S., Salvetti, A., Tognoni, E.: New procedure for quantitative elemental analysis by laser-induced plasma spectroscopy. *Appl. Spectrosc.* 53, 960–964 (1999).
<https://doi.org/10.1366/0003702991947612>
- Cremers, D.A., Ebinger, M.H., Breshears, D.D., Unkefer, P.J., Kammerdiener, S.A., Ferris, M.J., Catlett, K.M., Brown, J.R.: Measuring Total Soil Carbon with Laser-Induced Breakdown Spectroscopy (LIBS). *J. Environ. Qual.* 30, 2202–2206 (2001). <https://doi.org/10.2134/jeq2001.2202>
- Cuadri, A.A., Navarro, F.J., García-Morales, M., Bolívar, J.P.: Valorization of phosphogypsum waste as asphaltic bitumen modifier. *J. Hazard. Mater.* 279, 11–16 (2014).
<https://doi.org/10.1016/j.jhazmat.2014.06.058>
- Edwards, L., Winefordner, J.D.: Laser-Induced Breakdown Spectroscopy for the Determination of Carbon in Soil. *Chemistry (Easton)*. Ph.D., 140 (2007)
- Effenberger, A.J., Scott, J.R.: Effect of atmospheric conditions on LIBS spectra. *Sensors.* 10, 4907–4925 (2010). <https://doi.org/10.3390/s100504907>

Eseller, K.E., Yueh, F.Y., Singh, J.P., Melikechi, N.: Helium detection in gas mixtures by laser-induced breakdown spectroscopy. *Appl. Opt.* 51, (2012). <https://doi.org/10.1364/AO.51.00B171>

Farooq, W.A., Al-Johani, A.S., Alsalhi, M.S., Tawfik, W., Qindeel, R.: Analysis of polystyrene and polycarbonate used in manufacturing of water and food containers using laser induced breakdown spectroscopy. *J. Mol. Struct.* 1201, (2020). <https://doi.org/10.1016/j.molstruc.2019.127152>

Farooq, W.A., Al-Mutairi, F.N., Khater, A.E.M., Al-Dwayyan, A.S., AlSalhi, M.S., Atif, M.: Elemental analysis of fertilizer using laser induced breakdown spectroscopy. *Opt. Spectrosc. (English Transl. Opt. i Spektrosk.* 112, 874–880 (2012). <https://doi.org/10.1134/S0030400X12060082>

Farooq, W.A., Rasool, K.G., Tawfik, W., Aldawood, A.S.: Application of laser induced breakdown spectroscopy in early detection of red palm weevil: (*Rhynchophorus ferrugineus*) infestation in date palm. *Plasma Sci. Technol.* 17, 948–952 (2015). <https://doi.org/10.1088/1009-0630/17/11/11>

Farooq, W.A., Tawfik, W., Alahmed, Z.A., Ahmad, K., Singh, J.P.: Role of Purging Gases in the Analysis of Polycarbonate With Laser-Induced Breakdown Spectroscopy. *J. Russ. Laser Res.* 35, 252–262 (2014). <https://doi.org/10.1007/s10946-014-9420-9>

Farooq, W.A., Tawfik, W., Atif, M., Alsalhi, M.S., Zahran, H.Y., Abd El-Rehim, A.F., Yahia, I.S., Mansoor, S.: Evaluation of laser Induced Breakdown Spectroscopy for analysis of annealed Aluminum Germanium alloy at different temperatures. *IOP Conf. Ser. Mater. Sci. Eng.* 383, (2018). <https://doi.org/10.1088/1757-899X/383/1/012012>

Fikry, M., Tawfik, W., Omar, M.: Measurement of the Electron Temperature in a Metallic Copper Using Ultrafast Laser-Induced Breakdown Spectroscopy. *J. Russ. Laser Res.* 41, 484–490 (2020)(a). <https://doi.org/10.1007/s10946-020-09901-w>

Fikry, M., Tawfik, W., Omar, M.M.: Investigation on the effects of laser parameters on the plasma profile of copper using picosecond laser induced plasma spectroscopy. *Opt. Quantum Electron.* 52, (2020)(b). <https://doi.org/10.1007/s11082-020-02381-x>

Galbács, G.: A critical review of recent progress in analytical laser-induced breakdown spectroscopy. *Anal. Bioanal. Chem.* 407, 7537–7562 (2017). <https://doi.org/10.1007/s00216-015-8855-3>

Gallou, C., Pailloux, A., Lacour, J.L.: Chemical warfare detection by LIBS. 30, 263–270 (2009)

Gojani, A.B.: Experimental Study of Laser-Induced Brass and Copper Plasma for Spectroscopic Applications. *ISRN Spectrosc.* 2012, 1–8 (2012). <https://doi.org/10.5402/2012/868561>

Griem, H.R.: *Plasma Spectroscopy*. McGraw-Hill (1964)

Harmon, R.S., Lawley, C.J.M., Watts, J., Harraden, C.L., Somers, A.M., Hark, R.R.: Laser-induced breakdown spectroscopy-An emerging analytical tool for mineral exploration. *Minerals.* 9, 1–45 (2019).

<https://doi.org/10.3390/min9120718>

J. J, E.: Elemental Composition of Selected Inorganic Fertilizers in Zaria by XRF Method: A Source of Possible Environmental Contamination. *IOSR J. Appl. Chem.* 7, 01–03 (2014).

<https://doi.org/10.9790/5736-07420103>

Ji, G., Ye, P., Shi, Y., Yuan, L., Chen, X., Yuan, M., Zhu, D., Chen, X., Hu, X., Jiang, J.: Laser-induced breakdown spectroscopy for rapid discrimination of heavy-metal-contaminated seafood *Tegillarca granosa*. *Sensors (Switzerland)*. 17, 1–11 (2017). <https://doi.org/10.3390/s17112655>

Kaski, S., Häkkänen, H., Korppi-Tommola, J.: Laser-induced plasma spectroscopy to as low as 130 nm when a gas-purged spectrograph and ICCD detection are used. *Appl. Opt.* 42, 6036 (2003).

<https://doi.org/10.1364/ao.42.006036>

Kim, Y.K., Desclaux, J.P.: Ionization of carbon, nitrogen, and oxygen by electron impact. *Phys. Rev. A - At. Mol. Opt. Phys.* 66, 127081–1270812 (2002). <https://doi.org/10.1103/PhysRevA.66.012708>

Kramida, A., Ralchenko, Y.: NIST ASD Output: Lines, NIST Atomic Spectra Database (2018).

Li, Y., Tian, D., Ding, Y., Yang, G., Liu, K., Wang, C., Han, X.: A review of laser-induced breakdown spectroscopy signal enhancement. *Appl. Spectrosc. Rev.* 53, 1–35 (2018).

<https://doi.org/10.1080/05704928.2017.1352509>

Liu, H.C., Mao, X.L., Yoo, J.H., Russo, R.E.: Early phase laser induced plasma diagnostics and mass removal during single-pulse laser ablation of silicon. *Spectrochim. acta, Part B At. Spectrosc.* 54, 1607–1624 (1999). [https://doi.org/10.1016/S0584-8547\(99\)00092-0](https://doi.org/10.1016/S0584-8547(99)00092-0)

Marangoni, B.S., Silva, K.S.G., Nicolodelli, G., Senesi, G.S., Cabral, J.S., Villas-Boas, P.R., Silva, C.S., Teixeira, P.C., Nogueira, A.R.A., Benites, V.M., Milori, D.M.B.P.: Phosphorus quantification in fertilizers using laser induced breakdown spectroscopy (LIBS): A methodology of analysis to correct physical matrix effects. *Anal. Methods*. 8, 78–82 (2016). <https://doi.org/10.1039/c5ay01615k>

Merk, S., Scholz, C., Florek, S., Mory, D.: Increased identification rate of scrap metal using Laser Induced Breakdown Spectroscopy Echelle spectra. *Spectrochim. Acta - Part B At. Spectrosc.* 112, 10–15 (2015).

<https://doi.org/10.1016/j.sab.2015.07.009>

Mortazavi, S.Z., Parvin, P., Mousavi Pour, M.R., Reyhani, A., Moosakhani, A., Moradkhani, S.: Time-resolved evolution of metal plasma induced by Q-switched Nd:YAG and ArF-excimer lasers. *Opt. Laser Technol.* 62, 32–39 (2014). <https://doi.org/10.1016/j.optlastec.2014.02.006>

Nizevičienė, D., Vaičiukynienė, D., Michalik, B., Bonczyk, M., Vaitkevičius, V., Jusas, V.: The treatment of phosphogypsum with zeolite to use it in binding material. *Constr. Build. Mater.* 180, 134–142 (2018).

<https://doi.org/10.1016/j.conbuildmat.2018.05.208>

Pacheco-Torgal, F., Ding, Y., Miraldo, S., Abdollahnejad, Z., Labrincha, J.A.: Are geopolymers more suitable than Portland cement to produce high volume recycled aggregates HPC? *Constr. Build. Mater.* 36, 1048–1052 (2012). <https://doi.org/10.1016/j.conbuildmat.2012.07.004>

Palleschi, V.: Laser-induced breakdown spectroscopy: principles of the technique and future trends. *ChemTexts.* 6, 1–16 (2020). <https://doi.org/10.1007/s40828-020-00114-x>

Potiriadis, C., Koukoulidou, V., Seferlis, S., Kehagia, K.: Assessment of the occupational exposure at a fertiliser industry in the northern part of Greece. *Radiat. Prot. Dosimetry.* 144, 668–671 (2011). <https://doi.org/10.1093/rpd/ncq309>

Qi, H., Lai, H.: Micromachining of Metals and Thermal Barrier Coatings using a 532 nm Nanosecond Fiber Laser. *Phys. Procedia.* 39, 603–612 (2012). <https://doi.org/10.1016/j.phpro.2012.10.079>

Raciukaitis, G., Brikas, M., Gedvilas, M.: Efficiency aspects in processing of metals with high-repetition-rate ultra-short-pulse lasers. *ICALEO 2008 - 27th Int. Congr. Appl. Lasers Electro-Optics, Congr. Proc.* 403, 176–184 (2008). <https://doi.org/10.2351/1.5061377>

Rai, A.K., Zhang, H., Yueh, F.Y., Singh, J.P., Weisburg, A.: Parametric study of a fiber-optic laser-induced breakdown spectroscopy probe for analysis of aluminum alloys. *Spectrochim. Acta - Part B At. Spectrosc.* 56, 2371–2383 (2001). [https://doi.org/10.1016/S0584-8547\(01\)00299-3](https://doi.org/10.1016/S0584-8547(01)00299-3)

Rajavelu, H., Vasa, N.J., Seshadri, S.: Effect of ambiance on the coal characterization using laser-induced breakdown spectroscopy (LIBS). *Appl. Phys. A Mater. Sci. Process.* 126, 1–10 (2020). <https://doi.org/10.1007/s00339-020-03558-7>

Raven, K.P., Loeppert, R.H.: Trace Element Composition of Fertilizers and Soil Amendments. *J. Environ. Qual.* 26, 551–557 (1997). <https://doi.org/10.2134/jeq1997.00472425002600020028x>

Sabsabi, M.: Femtosecond LIBS. In: *Laser-Induced Breakdown Spectroscopy*. pp. 151–171. Elsevier Inc. (2007)

Şen, İ.: Spectroscopic Determination of Major Nutrients (N, P, K) of Soil. *Izmir Institute of Technology* (2003)

El Sherbini, A.M., El Sherbini, T.M., Hegazy, H., Cristoforetti, G., Legnaioli, S., Palleschi, V., Pardini, L., Salvetti, A., Tognoni, E.: Evaluation of self-absorption coefficients of aluminum emission lines in laser-induced breakdown spectroscopy measurements. *Spectrochim. Acta - Part B At. Spectrosc.* 60, 1573–1579 (2005). <https://doi.org/10.1016/j.sab.2005.10.011>

Tawfik, W., Bousiakou, L.G., Qindeel, R., Farooq, W.A., Alonizan, N.H., Fatani, A.J.: Trace analysis of heavy metals in groundwater samples using laser induced breakdown spectroscopy (LIBS). *Optoelectron. Adv. Mater. Rapid Commun.* 9, 185–192 (2015)(a)

Tawfik, W., Farooq, W.A., Al-Mutairi, F.N., Alahmed, Z.A.: Monitoring of inorganic elements in desert soil using laser-induced breakdown spectroscopy. *Lasers Eng.* 32, 129–140 (2015)(b)

Tawfik, W., Mohamed, Y.: Calibration free laser-induced breakdown spectroscopy (LIBS) identification of seawater salinity. *Opt. Appl.* Vol. 37, 5–19 (2007)

Unnikrishnan, V.K., Alti, K., Kartha, V.B., Santhosh, C.: V. K. Unnikrishnan, Kamlesh Alti, V. B. Kartha, C. Santhosh, G. P. Gupta and B. M. Suri, "Measurements of plasma temperature and electron density in laser-induced copper plasma by time-resolved spectroscopy of neutral atom and ion emissions", *Pramana Jour. Pramana –journal Phys.* 74, 983–993 (2010)

Welander: Einige Worte über die Form der Anwendung des Quecksilbers. *Arch. Dermatol. Syph.* 46, 476 (1898). <https://doi.org/10.1007/BF01825086>

Yueh, F.Y., Sharma, R.C., Singh, J.P., Zhang, H., Spencer, W.A.: Evaluation of the Potential of Laser-Induced Breakdown Spectroscopy for Detection of Trace Element in Liquid. *J. Air Waste Manag. Assoc.* 52, 1307–1315 (2002). <https://doi.org/10.1080/10473289.2002.10470860>

Zavilopulo, A.N., Chipev, F.F., Shpenik, O.B. 50, 402–407 (2005)

Table

Table 1 can be found in the Supplemental Files section.

Figures

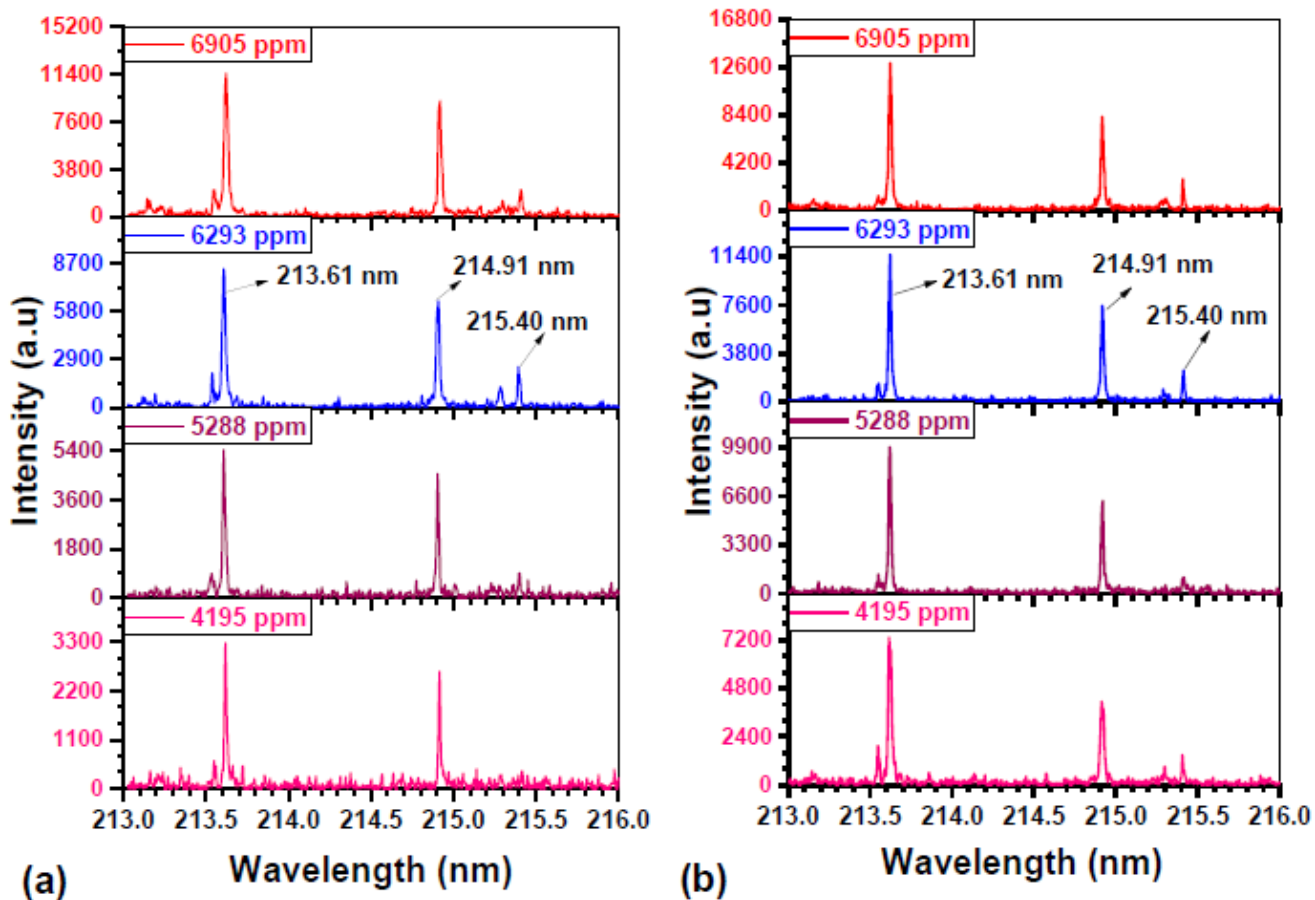


Figure 1

LIBS emission spectra using NIR laser 1064 nm at pulse energies of 50 mJ of different phosphogypsum samples (a) non-purged and (b) purge.

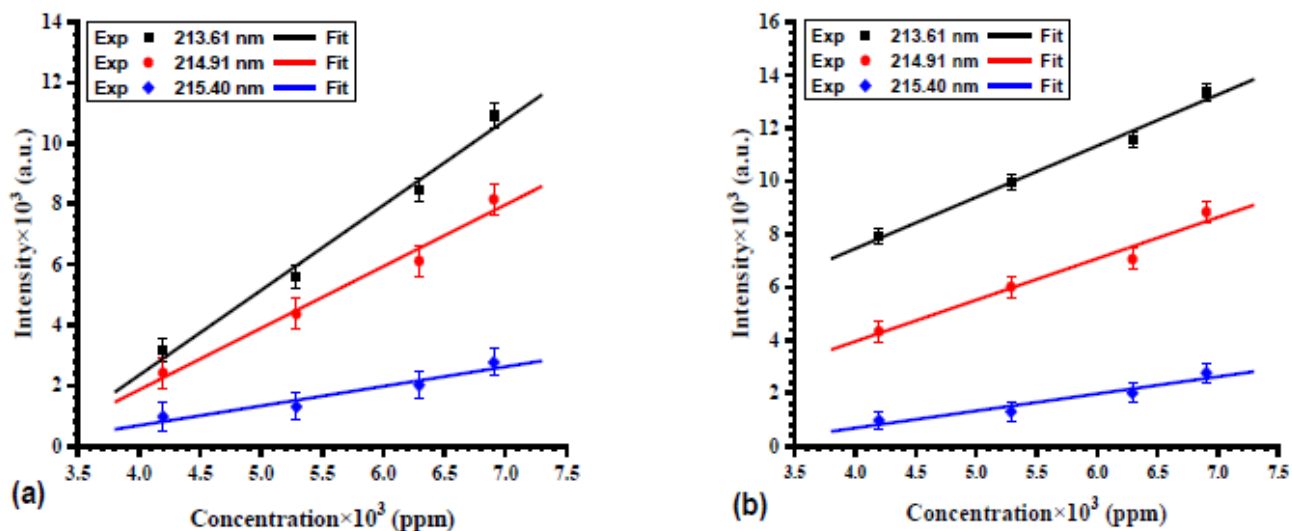


Figure 2

LIBS concentration calibration curve of P in different phosphogypsum samples (a) Non-purged and (b) Purge using NIR laser 1064 nm at pulse energies of 50 mJ.

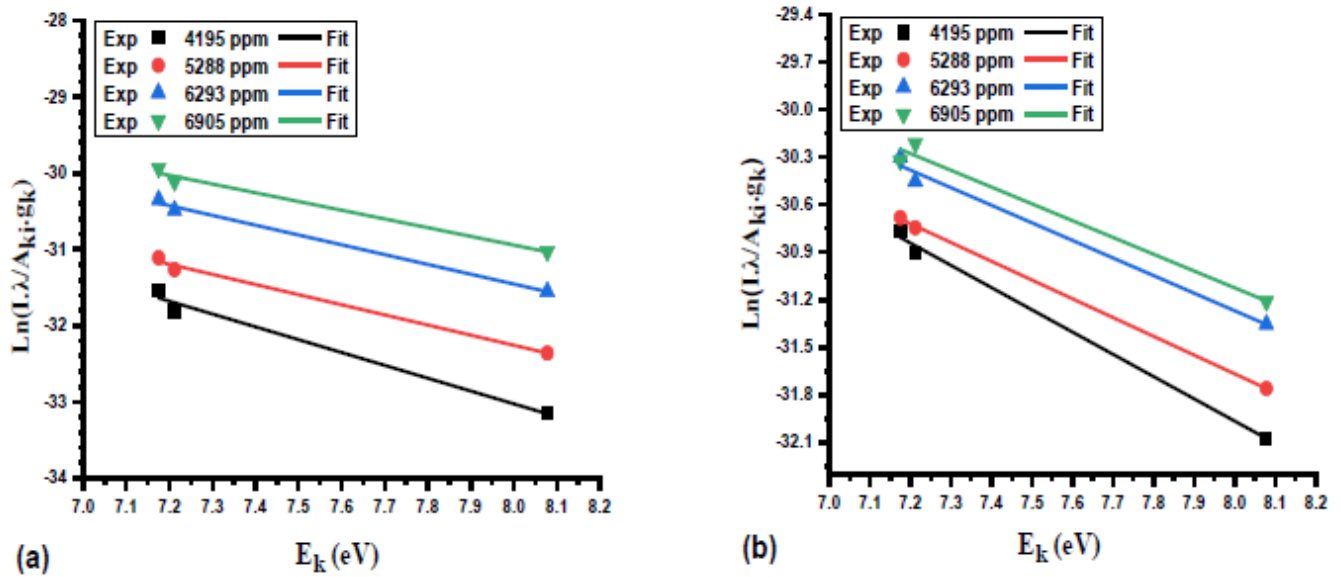
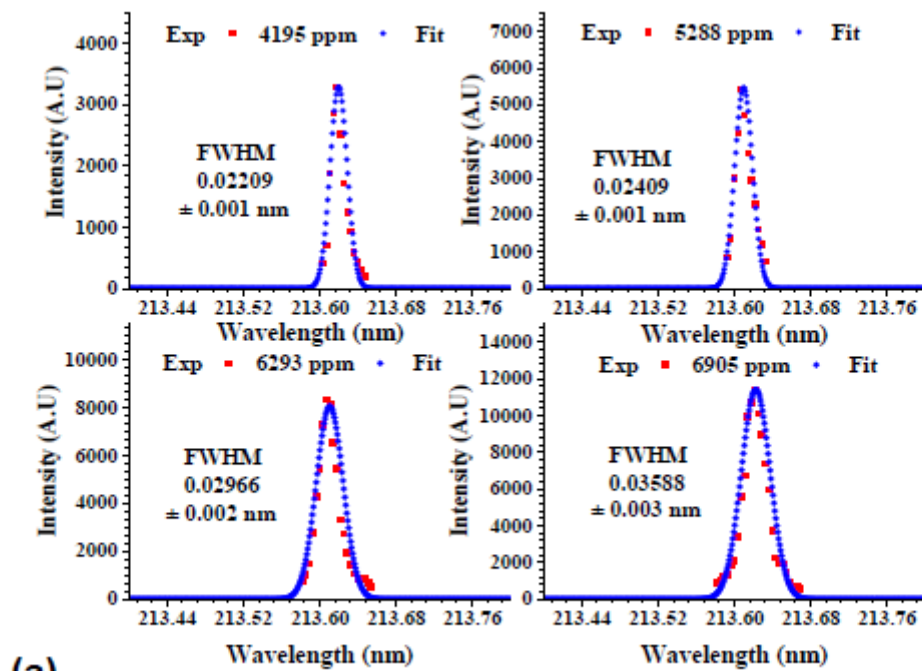
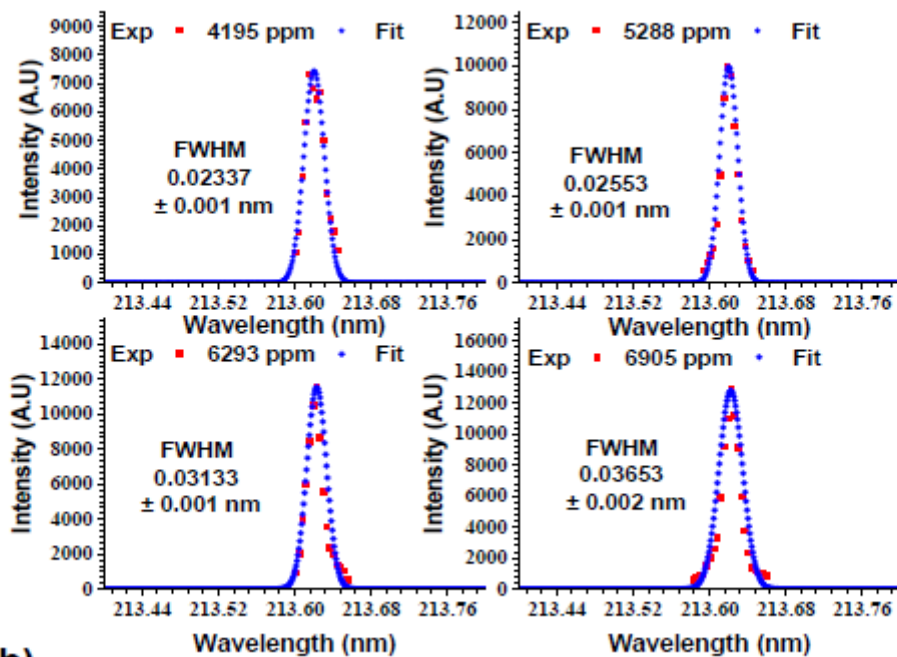


Figure 3

A Boltzmann plots for the P I lines (213.61, 214.91, 215.40 nm) in different concentrations of phosphogypsum samples (a) Non-purged and (b) Purged using NIR laser 1064 nm at pulse energies of 50 mJ.



(a)



(b)

Figure 4

Voigt Line profile of P I line 213.61 nm in different concentration phosphogypsum samples (a) Non-purged and (b) Purged using NIR laser 1064 nm at pulse energies of 50 mJ.

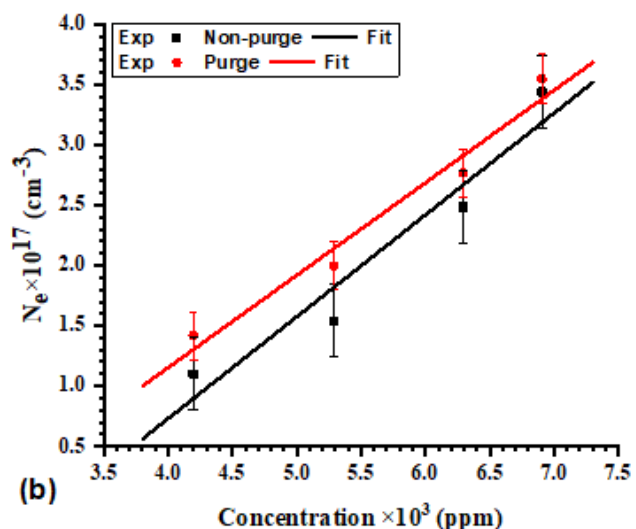
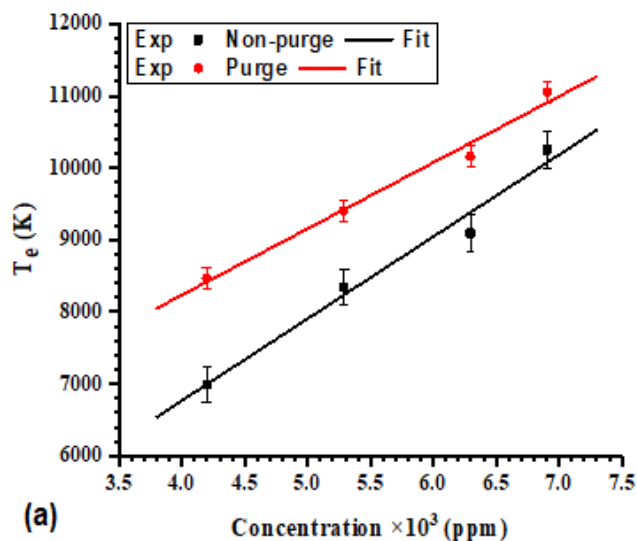


Figure 5

LIBS plasma electron temperature (T_e) (a) and electron density (N_e) at 213.61 nm (b) calibration curves for the P I lines in different phosphogypsum samples non-purged and purged using NIR laser 1064 nm at pulse energies of 50 mJ.

Supplementary Files

This is a list of supplementary files associated with this preprint. Click to download.

- [Table1.pdf](#)